Indian Journal of Engineering & Materials Sciences
Vol. 26, October-December 2019, pp. 390-402

# Physico-mechanical flammability and leachability characteristics of fly ash/slag based foamed geo polymer concrete blocks

Sandhya Deshwal[a], Brijeshwar Singh[a]*, Ishwarya Ganeshan[a] & Hina Tarannum[b]

[a]Polymer, Plastic & Composites Division, CSIR-Central Building Research Institute, Roorkee 247 667, India

[b]Department of Chemistry, Taibah University, Yanbu, KSA

*Received: 16 October 2018; Accepted: 26 July 2019*

*In-situ* foamed geo polymers have been produced from fly ash/slag blend, surfactant, hydrogen peroxide ($H_2O_2$) and sodium silico fluoride in an alkaline medium and evaluated their physico-mechanical, micro structural and fire characteristics as a function of foaming agent. Isothermal calorimetric response has been indicated that the rate of geo polymerization for the foam slurry was ~25% more than its un-foam slurry. An increase of $H_2O_2$ from 0.5 to 3 wt% has reduced the compressive strength of foamed geo polymers from 7.2 to 2.45 MPa. As observed in field emission scanning electron microscope (FESEM), the pores have been spherical ranging in sizes between 42 µm and 585 µm with varying $H_2O_2$ dosages. The relationship between the compressive strength and porosity has been in agreement with the exponential model. The thermal conductivity of foamed geo polymers has ~36% less than the commercial cellular concrete at a density of 1000 Kg/m$^3$. Flammability test has shown that the samples belong to D class as per ISO 11925-2 and also exhibiting no support to the fire growth when tested as per BS 476-6. During immersion in water, the alkali leaching (pH 11-12.2) and also the fractional release of Na (22 ppm) and Si (18 ppm) under TCLP test have been observed. Based on the results, the foamed geo polymer blocks have been produced with satisfactory properties as per the requirements of commercial specification of cellular concrete blocks.

**Keywords:** Geopolymer foam, Fly ash, Blocks, Compressive strength, Thermal conductivity

## 1 Introduction

In recent years, it is constant desire to develop light-weight building materials as the energy efficiency has become a more widespread concern[1,2]. The benefits of using these materials as non-load bearing walls in RCC/steel framed structures arise from their low dead load, low thermal conductivity, faster construction, lower haulage and handing cost. Various methods[3,4] have been considered to produce light-weight materials either by the chemical expansion/physical foaming (metallic aluminum powder, hydrogen peroxide, pre-formed foaming etc.) in the cement slurry or by introducing light-weight aggregates (expanded polystyrene beads, perlite etc.) in the pastes/mortars. In order to fulfill the acceptable end use requirements, the control on the pore size and its distribution is very important in the production of foamed concrete as the porosity determines its density and strength. Considering the fact that the polymer foams widely used today are prone to fire and release toxic gases during burning and the inorganic foams (refractory) need complex processing at higher temperature[5], it is therefore, essentially desirable to produce foamed concrete based on newer materials especially activated fly ash (geopolymer) with the added advantage of sustainability characteristics by using industrial by-products as precursor materials.

Geopolymers are an amorphous alumino silicate with a repeating unit of sialate monomer (-Si-O-Al-O-)[6]. They are produced by the reaction between the alumino silicate powders (fly ash, metakaolin etc.) and alkali hydroxides/alkali silicates. Due to advantageous properties such as high early strength, low water permeability and high chemical & temperature resistance, geopolymer is increasingly considered as an attractive alternative to Portland cement[7]. Foamed geopolymers constitute a recent research field in this direction with huge potential in the development of thermo-acoustic materials[1]. Several works[8-12] have been reported on the process of forming air bubbles in the fresh geopolymer pastes or mortars based on fly ash/metakaolin to display properties that are analogous or even better to conventional foamed concrete. Zhang *et al.*[8] produced

*Corresponding author (E-mail: singhb122000@yahoo.com)

geopolymer foams using class F fly ash though preformed foaming process with a diluted surfactant solution. The resultant foams exhibit a dry density of 850-950 Kg/m$^3$ and a compressive strength of 4-9 MPa depending on the type and dosage of alkali activator. Al Bakri Abdullah *et al.*[9] used preformed foaming process to produce heat-cured geopolymer foam based on class C fly ash, with a density of 1650 kg/m$^3$ and a compressive strength of 18 MPa. Abdollahnejad *et al.*[10] developed fly ash-based geopolymer foam using sodium perborate as a foaming agent at the activator-binder ratio of 0.8. The foamed geopolymer has a thermal conductivity of 0.1 $Wm^{-1}K^{-1}$ and a compressive strength of 6 MPa. Boke *et al.*[11] producedfly ash-based geopolymer foams using sodium hypochloride as a foaming agent at 90° C for use as fire proof insulation, internal wall and ceiling tiles. The foam has a porosity of 55% with a compressive strength of 3.1 MPa. The metakaolin-based geopolymer foam using silica fume as a foaming agent can be considered as an economical insulating material with a thermal[12] conductivity less than 0.2 $Wm^{-1}K^{-1}$. A number of studied have also reported on the microstructural examination of geopolymer foams in terms of pore size & its distribution, pore coalescence, cell shape and intercellular space[8,11-14]. Zhang *et al.*[8] in their findings revealed that the void sizes in the fly ash-based foams are predominantly in the diameter range of 50-400 μm with an average roundness factor of 0.6. Papa *et al.*[12] found that metakaolin-based foams have spherical shape pores with thick struts having a size distribution of 100-600 μm. These thick struts are beneficial to obtain desired mechanical strength of geopolymer foams. Controlling pore sizes of < 1mm in geopolymer foams can be done by maintaining the proper rheology of their slurries, correct dosage of foaming agent& activator and curing[14].

A review of fire behavior[15] revealed that geopolymers have excellent potential in many applications contrary to that of traditional insulating materials where high use temperature is anticipated (800-1000 °C). Fly ash-based geopolymers show good retention of strength upto 400 °C and a strength increase after heating[16] at 800 °C. The formation of crystalline nepheline phase and the broadening of characteristic quartz and mullite peaks due to partial amorphization at higher temperature may contribute to the good post-exposure strength[17]. Papakonstantinou *et al.*[18] studied fire performance of lightweight geopolymers using expanded polystyrene beads and ceramic spheres as aggregates. Based on the heat release rate and NBS smoke burner tests, these geopolymeric materials satisfied the flammability requirements of the Federal Aviation Administration (50 kw/m$^2$ incident heat flux). Lyon *et al.*[19] evaluated the fire response of geopolymer matrix carbon fiber composites under 50 KW/m$^2$ heat flux irradiance level. They found that composites did not ignite or release any smoke even after extended heat flux exposure and retains 60% of its original flexural strength after a simulated large fire exposure. The adequate retention of strength and non-combustibility of geopolymers makes its suitable for making fire resistant building elements.

The main concern of geopolymer foams is their stability under use conditions in view of leachability of their constituent skeleton materials. Musci *et al.*[20] used toxicity characteristic leaching procedure (TCLP) to assess the mobility of analytes from fly ash-based geopolymers and found that Si, Al, Fe and Ca are built well in the structures. Temuujin *et al.*[21] investigated leaching behavior of fly ash-based geopolymers cured at 600 °C using EPA 1131 method (TCLP). They found that the solubility of the Al, Si and Fe ions in 14 M NaOH and 18% HCl after 5 days immersion decreased from 1.3 to 16 fold in comparison to ambient cured geopolymers. It is also reported[22,23] that the trace elements such as Pb, As, Cu, Cd, Sn, Hg etc. present in the raw fly ashes are suitably immobilized in the geopolymer structures through physical encapsulation. An optimal mix with proper curing is essential in order to obtain a long term stable final geopolymeric products.

Although in prior art, most works have been focused on heat cured fly ash-based foamed geopolymers, there have been limited reports available on the near ambient cured fly ash/slag-based foamed geopolymers with the combined use of surfactant and foaming agent. From a practical application point of view, some aspects such as control of bubbles coalescence, geopolymerization reaction in the presence of foaming agents and related manufacturing issues are still requiring attention for foamed geopolymer based product development. In the present work, in-situ geopolymer foams were produced using fly ash/slag blend and the combined use of surfactant and different dosages of $H_2O_2$. The use of surfactant aimed at to stabilize the foaming procedure, reducing the pore collapse and coalescence when the foam is still in the liquid state. The compressive

strength, microstructure, thermal conductivity and fire characteristics of these foamed geopolymers were discussed. The leachability of alkali in water and fractional release of elements from the foamed geopolymers using toxicity characteristic leaching procedure was also reported. Based on this, foamed geopolymer concrete blocks were produced and their suitability was assessed according to Indian standard specification.

## 2 Materials and Methods

### 2.1 Materials

The fly ash collected from a coal fired National Thermal Power Station at Dadri, was used as a main raw material to produce geopolymers. The fine fly ash retained ~24 % on a 45 µm sieve whereas, the coarse ash retained ~43 % of its total mass which is outside the specification range (34%) of IS: 3812[24].The mean particle size and Blaine's surface area of fly ash were ~21.03 µm and ~350$m^2$/kg, respectively. Ground granulated blast furnace slag, a by-product of pig iron manufacturing was collected from M/s Rashtriya Ispat Nigam Limited, Vishakhapatnam. The mean particle size and Blaine's surface area of slag were ~15.16 µm and ~514$m^2$/kg, respectively. The chemical composition of fly ash and slag analyzed by the X-ray Fluorescence Spectrometer is given in Table 1. The scanning electron microscopic images shows that fly ash particles were rounded with a smooth surface while the particles of slag were angular with a rough surface (Fig. 1(a & b)). The particle size distribution of fly ash, slag and their blend is shown in Fig. 2. Laboratory grade sodium hydroxide (Thomas Baker, purity 99.5%) and commercial sodium silicate ($Na_2O$: 14.5%, $SiO_2$: 29%, and water: 55%) were used as activators. Sodium lauryl sulphate (Thomas Baker, molecular weight, 288.38) and hydrogen peroxide (Thomas Baker, $H_2O_2$ 30% w/w concentration) were

Table 1 — Chemical composition of fly ash and ground granulated blast furnace slag.

| Oxide (wt%) | Fly ash (%) | Slag (%) |
|---|---|---|
| $SiO_2$ | 56.95 | 31.90 |
| $Al_2O_3$ | 31.17 | 16.17 |
| CaO | 1.416 | 40.73 |
| $Fe_2O_3$ | 5.04 | 0.86 |
| MgO | 0.464 | 6.519 |
| $SO_3$ | 0.13 | 1.32 |
| MnO | 0.03 | 0.07 |
| $Na_2O$ | 0.078 | 0.202 |
| $K_2O$ | 1.414 | 0.64 |
| $TiO_2$ | 2.39 | 0.89 |
| LOI* | 0.92 | 0.69 |

*Loss on ignition

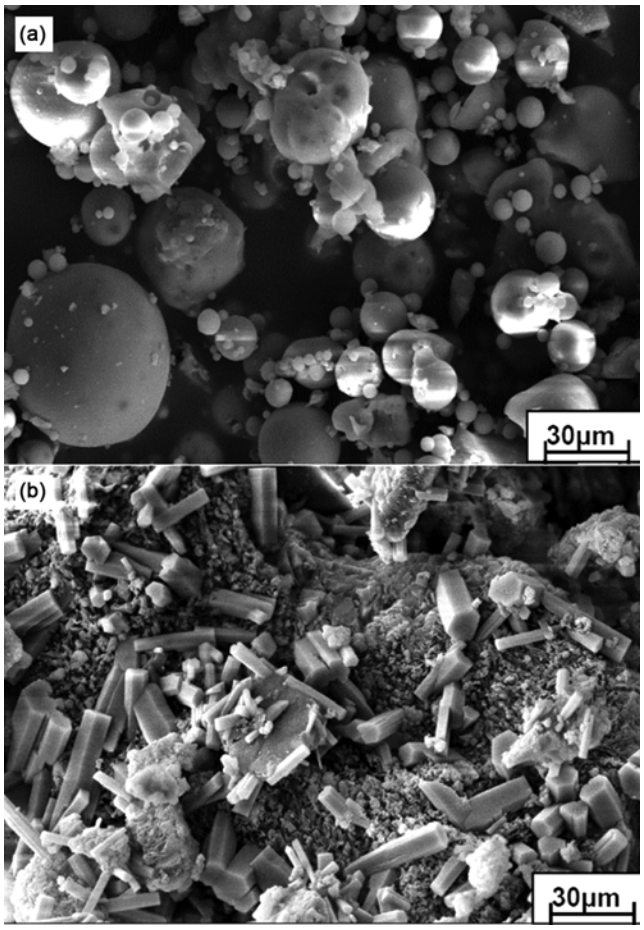


Fig. 1 — FE-SEM images of (a) fly ash and (b) ground granulated blast furnace slag.

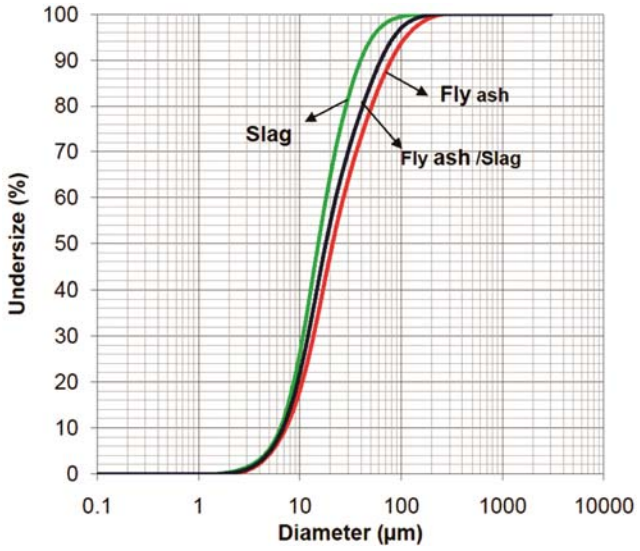


Fig. 2 — Particle size distribution of fly ash, slag and their mix.

used as surfactant and foaming agent respectively. Sodium silicofluoride (Lobachemie, molecular weight, 188.50) was used as a setting hardener in the mix.

**2.2 Sample preparation**

Fly ash and slag were initially dried in an oven at 100 ± 5 °C for 24h to remove their surface moisture. Thereafter, these were proportioned in a ratio of 80:20 as optimized earlier[25] and inter-ground in a planetary ball mill (Retsch PM-400) at 80 RPM for 5 min keeping the tungsten carbide ball-material ratio of 1:1. The resulting mix has a mean particle size of ~18.02 μm as obtained by a particle size analyzer. Activating solution was prepared by the blending of sodium hydroxide (12M) and sodium silicate solutions in a ratio of 1:2.5 (mass ratio). The water content in the activator was in the range of 58-60%. The resulting solution was then cooled for 24 h prior to its use.

In-situ geopolymer foam was produced using fly ash/slag blend, activating solution, foaming agent, surfactant and setting hardener. The fly ash /slag blend and activating solution (45-48 wt%) were thoroughly mixed in a laboratory mixer for 5 min to obtain a homogeneous paste slurry. Thereafter, sodium lauryl sulphate (~0.3 wt%) and $H_2O_2$ (0.5-3 wt%) were added to the slurry and its stirring was continued for another 3 min. While stirring the slurry, sodium silico fluoride (~3 wt%)was added into it to accelerate the geopolymerization reaction. It is mentioned that adding sodium silico fluoride into slurry just prior to the casting operation makes the composition capable of rapid setting. The resulting foam slurry can be handled soon after being poured into a mould[14]. Delayed setting increases the possibility of joining bubbles and the development of interconnections between pores, and therefore increases the chance of developing open porosity**.** At a time of creaming, the slurry was poured into the 100 x100 x100 mm cube mould, kept at room temperature for 2 h and then transferred into an air circulating oven at 60 ± 2 °C for 2 h. Prior to casting, an emulsified wax (specific gravity: 0.8, pH: 6, and solid content: ~40%) was used as a mould releasing agent to obtain a smooth surface of samples with ease of release. The sample was then de-moulded and stored at room temperature for 28 days prior to testing.

**2.3 Methods**

*2.3.1 Isothermal conduction calorimetry*

The heat flow rate during the alkaline activation of fly ash/slag blend and its foam was measured according to method B of ASTM C1702on an Isothermal Conduction Calorimeter (TAM AIR, TA Instruments). Conditioning of both fly ash/slag blend and activator was done to the same temperature as the calorimeter within ± 0.2 °C before mixing. The sample was mixed in the vial outside the Calorimeter and then loaded intothe sample chamber within 2 min. Activator-binder ratio in the paste was kept at ~0.45. The test was performed at 25 °C for 7 days to record cumulative heat release during the formation of reaction products in the geopolymer pastes.

*2.3.2 Physico-mechanical tests*

The physical tests on the foamed samples such as bulk density, water absorption and drying shrinkage were performed as per IS:2185[26]. The bulk density of foamed geopolymers was determined by measuring their weight-to-volume ratio. As used earlier by several authors[12,27,28], the apparent porosity of foamed geopolymers was determined by ASTM C 20 using following formula:

$$P = \left[W - \frac{D}{V}\right] \times 100 \quad \ldots (1)$$

Where, P is apparent porosity, W is saturated weight, D is dry weight and V is exterior volume.

The water absorption was measured by recording changes in the weight of sample before and after immersion in water at room temperature for 24 h. The drying shrinkage was calculated as the difference between the original wet length measurement and dry length measurement by immersing the sample in water for 4 days followed by its drying at 100 ± 5 °C for 44 h in an air circulating oven. The results reported were the average of three specimens. Leachability of metals from the foamed geopolymers was estimatedby Toxicity Characteristic Leaching Procedure (TCLP:1311)[29]. The samples were ground and kept at 4 °C in a refrigerator. About 25 g of samples were placed in a flask containing 500 ml of extraction fluid (glacial acetic acid and 1N NaOH in distilled water) equal to 20 times the weight of the solid phase and agitated for 18 h using an electric vibrator. The slurry was filtered through a Millipore filter paper. The leachate was then analyzed by the ICP-MS technique for estimation of various cations (Na, Si, Al, Ca and Fe).

The thermal conductivity of foamed: geopolymer sheets (300 mm x300 mm x 30 mm) was measured according to IS 3346[30] using a Guarded Hot Plate Conductivity Apparatus. Two specimens as nearly

identical were mounted between the hot plate and cold plate with a good contact between each other. At steady state, measurements were taken at 30 min intervals until four successive sets of measurements gave thermal conductivity values differing by not more than 1%.

The compressive strength of 100 x 100 x 100 mm cube specimens was tested as per IS:1727[31] at a cross-head speed of 0.5 mm/min on a universal testing machine (Testometric, 50 KN). The load-deflection curve for each sample was recorded. The average result of three samples was reported.

*2.3.3 Field emission scanning electron microscopy*

The surface morphology of fly ash/slag particles and the fractured surface of geopolymer foam samples were examined on a field emission scanning electron microscope (FESEM, QUANTA). Prior to SEM examination, the samples were vacuum coated with a thin film of gold/palladium to render them conductive. Elemental mapping of the microstructure was also carried out by an energy dispersive spectroscopy attached to FESEM.

*2.3.4 Fire resistance test*

The ignitability test (single flame source) on the samples (250 mm x 90 mm x 30 mm) was carried out as per ISO: 11925-2. The flame duration was 60s from the time at which the flame is applied. Ignition of the filter paper and the time at which flame tip reached 150 mm at the flame application point were noted. The fire propagation test on the specimen of size 225 mm x 225 mm x 12 mm was conducted as per BS 476: Part-6. The test run was continued for 20 min duration. The result of fire propagation index was computed from the difference between the sample and the reference specimen using time-temperature curve of the test. The surface spread of flame test was carried out on a sample of size 270 mm x 900 mm x 15 mm according to BS 476: Part-7. Based on the extent and rate of flame spread, the categorization of sample for "Fire Class" was carried out. Cone Calorimeter (FTT Ltd.) was used to measure the flammability characteristics of foamed geopolymer samples (100 mm x100 mm x12 mm) according to ISO: 5660-1. The test was conducted for 20 min at a heat flux of 50 KW/m$^2$ and normal duct flow of 24l/s. Various parameters such as heat release rate, total smoke release, carbon monoxide (CO) yield, carbon dioxide ($CO_2$) yield, mass loss rate, and heat of combustion were recorded.

## 3 Results and Discussion

### 3.1 Calorimetric studies

Fig. 3 (a & b) shows the calorimetric responses of the activated fly ash and activated fly ash/slag blend with and without $H_2O_2$. The existence of a single peak in the curves corresponds to the overlapping of dissolution as well as condensation reactions. The heat evolution rate at peak for the activated fly ash was ~16.79 mW/g. When the slag was mixed into the fly ash, its heat flow rate reduced to ~12.06 mW/g probably the involvement of calcium ions released from the slag in the reaction process. Upon adding $H_2O_2$/surfactant into the activated fly ash/slag blend resulted in further decrease of heat evolution rate of the resulting mix (~11.80 mW/g). This decrease is

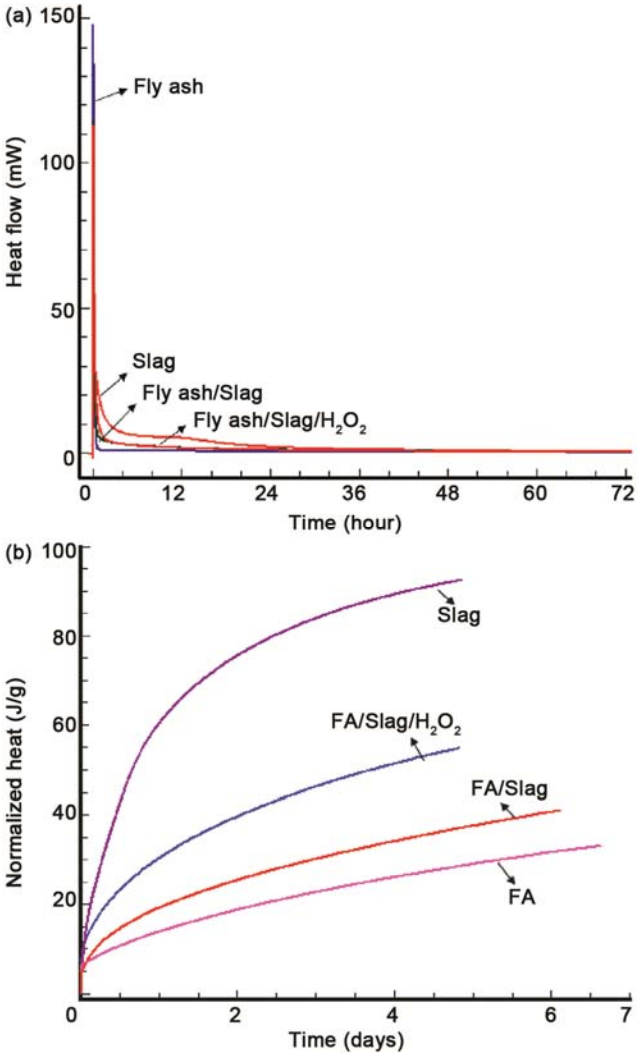


Fig. 3 — Isothermal calorimetric response of fly ash/slag based geopolymer pastes at 25 °C (a) Normalized heat flow curve and (b) Normalized heat.

attributed to the formation of initial unstable peroxide hydrate[32] ($Na_2SiO_3.xH_2O_2.yH_2O$, where x = 2.5-3, y = 0-1) as a result of molecular hydrogen bonding between the silanol groups of sodium silicate and $H_2O_2$which opposed dissolution process of fly ash/slag particles. It was observed that the heat flow rate of foamed paste in the post acceleration period was also higher than that of its un-foamed ones. The dormant period delayed as against its un-foamed counterpart. This delay may be considered due to the high water content in the foamed paste that probably obstructed its setting[5].

The total heat release obtained from the area of integration under the heat flow curve for fly ash paste was ~33.15 J/g only, whereas its mix with slag produced total heat release of ~ 41.09 J/g (Fig. 3(b)). Since slag alone had ~ 92.5 J/g total heat release during the activation, its contribution in the total heat of hydration of fly ash/slag paste appears to be significant. When the paste was foamed with $H_2O_2$/surfactant, the total heat release (~54.92 J/g) was higher than that of its un-foamed paste. While adding $H_2O_2$ into the slurry, the reaction was vigorous and $H_2O_2$ decomposed in a non-chain fashion[33]. The mixture of sodium hydroxide and $H_2O_2$ acted as a strong oxidizer and can result in an exothermic reaction in the slurry. This temperature rise due to exothermic effect (enthalpy: -98.2 KJ/mol) enhanced the geopolymerization reaction of fly ash/slag blend. The higher the heat of hydration of the paste, the higher is the formation of reaction products and consequently, the improvement in mechanical properties.

### 3.2 Physico-mechanical Properties

The effect of foaming agent ($H_2O_2$& surfactant) on the properties of fly ash/slag foamed geopolymers is given in Table 2. As the foaming dosage was increased, the cream time in the slurry got decreased and its volumetric expansion increased. It was observed that cream time in the slurry occurred within 2.2 min. The foam rise in the slurry was ~6 mm at 0.5 wt% $H_2O_2$ and it increased to ~29 mm at a level of 3 wt% $H_2O_2$. The density of foamed geopolymers varied from 700 to 1000 kg/m$^3$ with different $H_2O_2$ contents (0.5-3 wt%).As obtained by the water saturation method, the open porosity in the foamed geopolymers increased from 55.60% for 0.5 wt% $H_2O_2$ to 72.80% for 3 wt% $H_2O_2$content.The decomposition of $H_2O_2$ generated oxygen gas under the influence of an alkaline aqueous solution which formed bubbles/cells in the slurry resulting in lowering of the hardened mass density. As would be expected, the water absorption of samples increased with decreasing density (Fig. 4). The existence of interconnected pores may be considered responsible for more diffusion of water. When compared with the commercial specification of cellular cement concrete (IS: 2185, 2008), the foamed geopolymers had 35-50 % less water absorption.

As can be seen in Fig. 5, the initial slope of stress-strain curves varied with increasing foaming agent. The foamed geopolymer samples exhibited a post-peak behavior un-like the un-foamed samples because the foam cell deformed in a plastic manner[34].The specimens carried load even after the yield upto relatively large strains. The plasticity occurred in

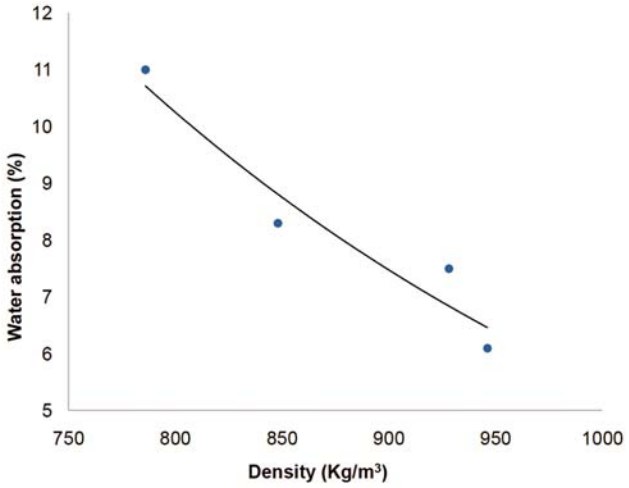


Fig. 4 — Water absorption of the foamed geopolymers as a function of density at room temperature.

Table 2 — Effect of $H_2O_2$ dosage on the physico-mechanical properties of foamed geopolymers.

| $H_2O_2$ (wt %) | Cream time (min) | Foam rise (mm) | Density (kg/m$^3$) | Pore size range (μm) | Open porosity (vol%) | Total porosity (%) | Water absorption (%,24h) | Compressive strength (MPa) | Thermal conductivity (Wm./K) |
|---|---|---|---|---|---|---|---|---|---|
| 0.5 | 2.1 | 6 | 1000 ± 50.00 | 42-205 | 31.75 ± 1.6 | 55.6 ± 2.78 | 6.1 ± 0.30 | 7.2 ± 0.36 | 0.228 ± 0.011 |
| 1 | 1.8 | 12 | 946 ± 47.30 | 105-385 | 47.07 ± 2.4 | 62.5 ± 3.12 | 8.3 ± 0.41 | 6.5 ± 0.32 | 0.213 ± 0.010 |
| 2 | 1.5 | 25 | 848 ± 42.40 | 140-428 | 65.68 ± 3.3 | 67.6 ± 3.38 | 19.4 ± 0.97 | 4.2 ± 0.21 | 0.181 ± 0.009 |
| 3 | 1.4 | 29 | 700 ± 35.00 | 217-585 | 70.81 ± 3.5 | 72.8 ± 3.64 | 27.6 ± 1.38 | 2.45 ± 0.12 | 0.158 ± 0.008 |

the foams is attributed to the incomplete geopolymerization reaction of fly ash/slag and also, the hindrance exerted by the closed cells for water removal during the curing process. The pore size distribution and the smaller pores are important in distributing the load inside the matrix and helped in achieving more strength[14]. The compressive strength of foamed geopolymers decreased with increasing foaming agent (Fig. 6). At 0.5 wt% $H_2O_2$, the compressive strength of foamed geopolymer was 7.2 MPa. When the $H_2O_2$ content was increased at a level of 3 wt%, the compressive strength dropped to 2.45 MPa. This can be explained with the help of the relationship between the compressive strength and porosity of foamed geopolymers using the minimum solid area modal proposed by Rice[35].

$$\sigma = \sigma_o e^{-bp} \quad \ldots (2)$$

where, σ is the strength of total porosity p, $\sigma_o$ is the strength of zero porosity (p=0) and b is a parameter determined by the character of the porosity. The b value obtained from the slope of compressive strength versus porosity plot was 6.31 (Fig. 7).This value is associated with the spherical pores (orientation related to the measuring direction). In general, the lower the slope (b value), the higher the critical porosity. As indicated by the higher $R^2$(0.888), the model fits reasonably good with the observed values (porosity range; 55-73 vol%). It can be seen that the difference between the observed and predicted values at lower porosity was relatively large. The larger pores affected more to the strength than the smaller pores in the foamed geopolymers. On comparing, it was observed that the compressive strength of specification grade fine fly ash-based foamed geopolymers was significantly higher than the coarse ash-based foams (Fig.8). The difference in the

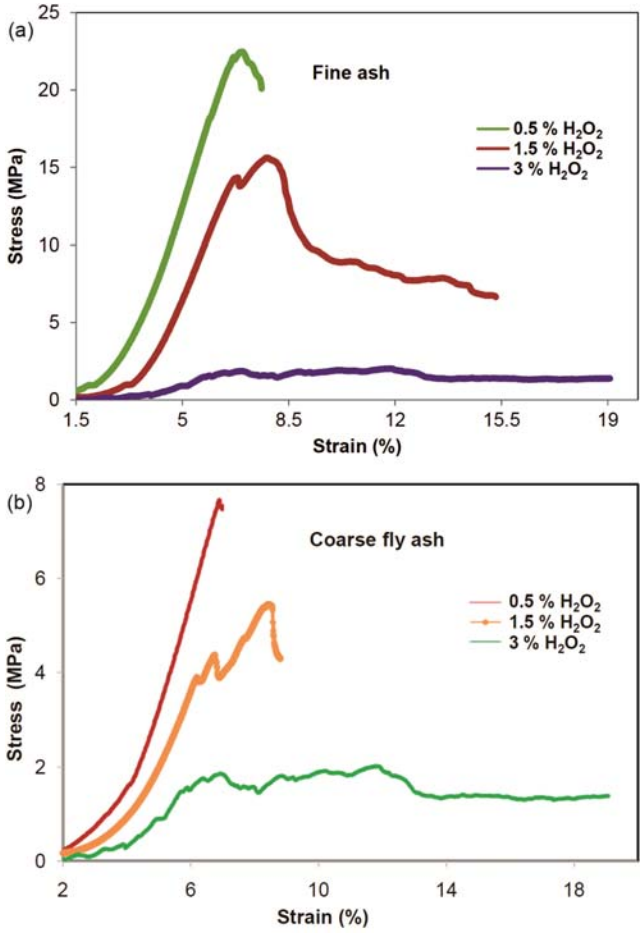


Fig. 5 — Compressive stress-strain curves of the foamed geopolymers (a) Fine ash and (b) Coarse ash.

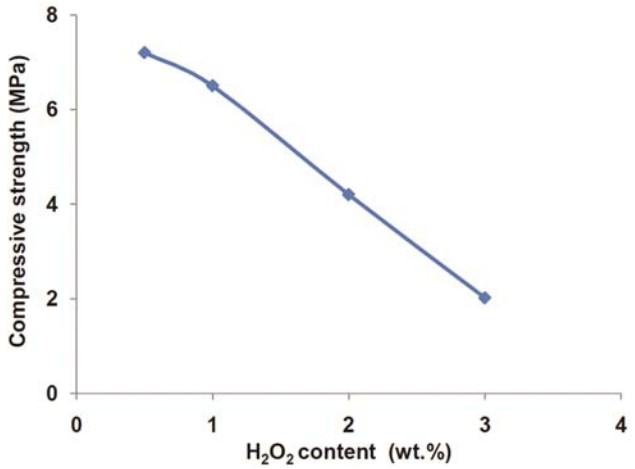


Fig. 6 — Compressive strength of the foamed geopolymers as a function of $H_2O_2$ content.

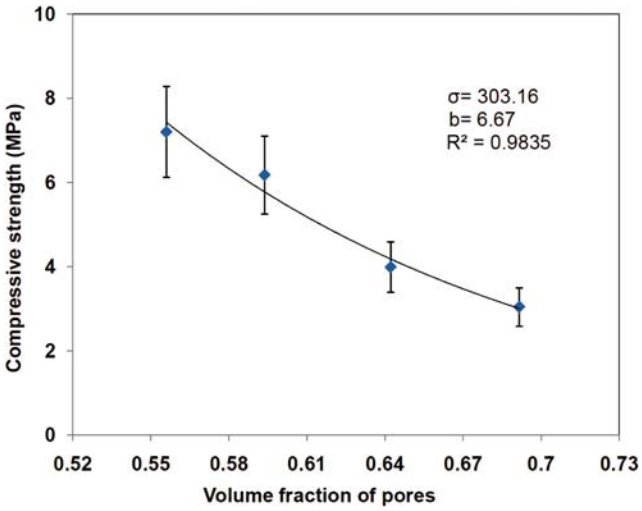


Fig. 7 — Compressive strength versus porosity of the foamed geopolymers.

strength is believed to be the formation of more reaction products (N-A-S-H and (Ca-Na)-A-S-H) as a result of greater rate of geopolymerization of fine fly ash than the coarse ash[36].

Backscattered images on the fractured surfaces of foamed geopolymers are shown in Fig. 9 (a-d). The pores were generally rounded in shape at 0.5 wt% $H_2O_2$.The most of the pores were distributed between

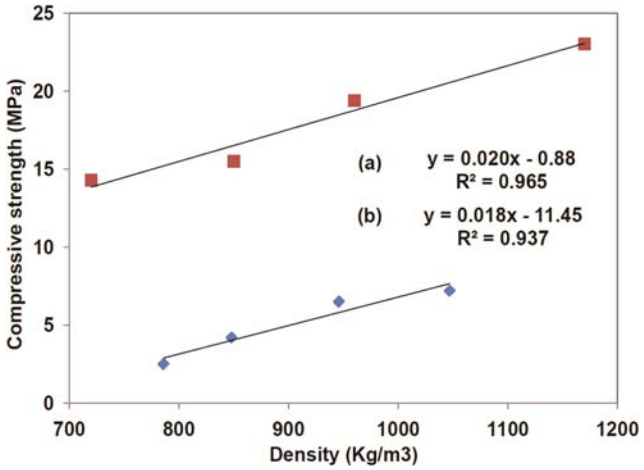


Fig. 8 — Compressive strength of the foamed geopolymers as a function of density content (a) Fine fly ash and (b) Coarse ash.

42µm and 205 µm as viewed in the image analysis. Above this level (1-3 wt% $H_2O_2$), the irregular shape pores were observed. The pores were thin walled with sizes ranging between 105 µm and 585 µm. The open porosity obtained by the image analysis increased significantly from 31.75 to 70.81 vol % when the $H_2O_2$ content increased from 0.5 wt% to 3 wt%. An increase of $H_2O_2$ content led to a decrease of slurry viscosity which involved pore coalescence resulting in larger pores[37]. When compared with the water saturation porosity, the porosity values obtained at higher $H_2O_2$ level were comparable. Contrary to this, the large difference in the values obtained by the both methods at lower $H_2O_2$ level was noted because image analysis cannot count smaller pores in the matrix. EDAX results of geopolymer matrix indicated that Ca/Si ratio and Si/Al ratio were 0.12-0.10 and 2.06-2.98 respectively. The low value of Ca/Si ratio compared to Portland cement (1.5-2.0) indicated that there has been some sodium replacing calcium in C-A-S-H phase supporting the existence of (Ca-Na)-A-S-H in the geopolymer[38]. Higher Si/Al ratio compared to raw fly ash (2.18) is attributed to the Si species added though sodium silicate activator. The

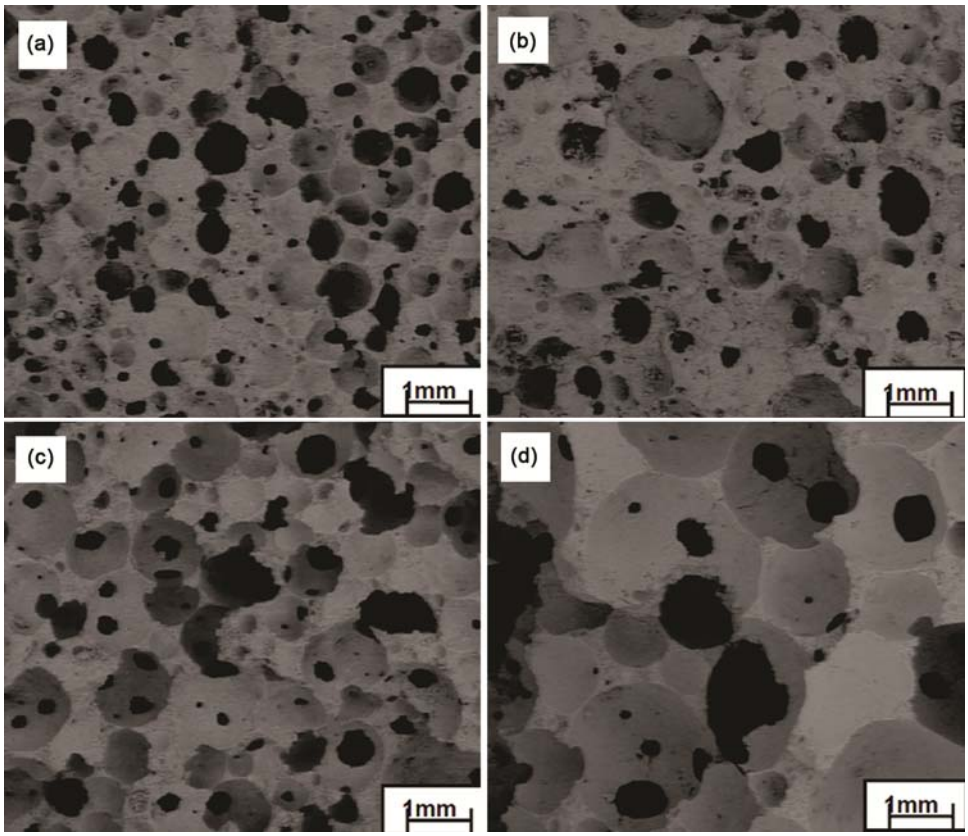


Fig. 9 — Backscattered images of foamed geopolymers at different $H_2O_2$ dosages (a) 0.5 wt%, (b) 1 wt%, (c) 2 wt% and (d) 3 wt%.

microstructures were also characterized by the presence of cracks, rounded structures and pore wall with the precipitates (Fig.10). The un-utilized sodium as observed in EDAX (22-25 wt%) was accumulated in the form of tubular round shaped structures in the paste (Fig. 10(a)) which may be responsible for carbonation of geopolymers by reacting with the atmospheric $CO_2$. The cracks were also viewed in the matrix (Fig.10 (b)) attributable to the silica-rich region and also the thermal stresses probably developed during the water evaporation from the pores. At some places, pore walls were porous mainly formed by the nano precipitation of reaction products (Fig.10c) due to the incomplete geopolymerization reaction of the fly ash/slag (Si/Al: 1.11, Ca/Si: 0.48, Na/Al: 0.299). Their presence increased the permeability of the structures. These factors affected significantly on the strength of the foamed geopolymers.

As can be seen in Fig. 11, the thermal conductivity of foamed geopolymers increased from 0.072 to 0.228 $Wm^{-1}K^{-1}$ when the oven dry density increased from 600 to 1000 $Kg/m^3$. As would be expected, the

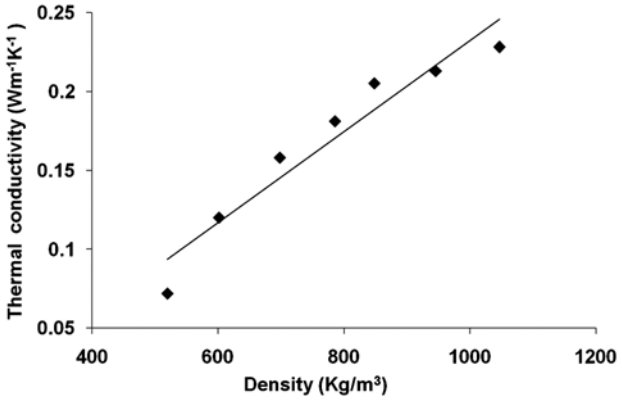


Fig. 11 — Thermal conductivity of the foamed geopolymers as a function of density.

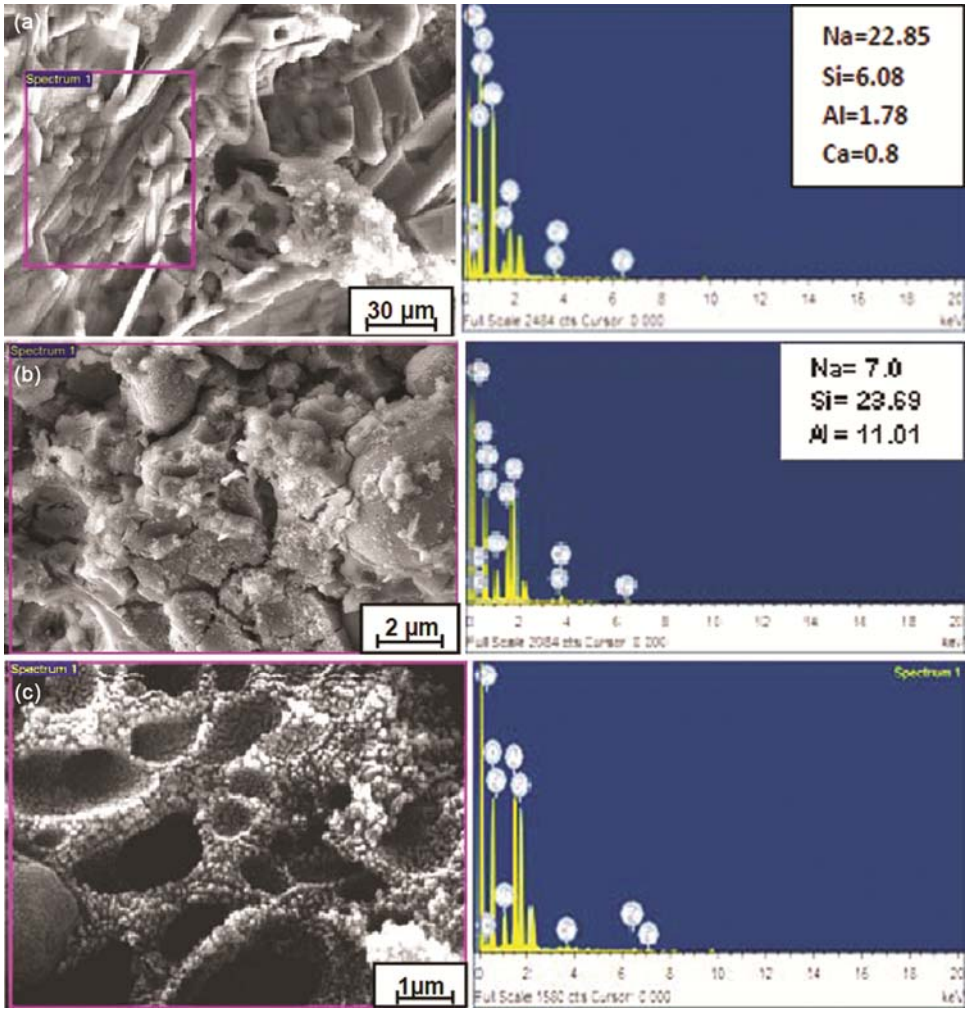


Fig. 10 — FESEM- EDAX images on the fracture surfaces of foamed geopolymers (a) Accumulation of sodium, (b) Crack appeared in the matrix and (c) Pore wall with the precipitated reaction products.

lower the density of foamed geopolymers, the lower is the thermal conductivity possibly due to the large number of voids and the low binder content[26]. Above ~700 Kg/m$^3$, the increase in the value of thermal conductivity of the foams was relatively small (~13%) possibly due to the relative orientation and position of pores (layering of pores) in the specimens[14]. It was noted that thermal conductivity of the foamed geopolymers was lower than the values reported for the commercial specification of cellular and aerated concrete (0.21-0.42 Wm$^{-1}$K$^{-1}$) with the same density indicating their better thermal insulating properties. The difference can be explained in terms of lower in calcium, higher in silicon and also amorphousness of the geopolymer binder[39] with a more discontinuous gel structure.

### 3.3 Fire Behavior

The reaction to fire characteristics of the foamed geopolymers is summarized in Table 3. The sample was non-ignitable when tested it's either at edge or surfaces under a single flame source classifying to the ignitability class of D (ISO 11925-2). During the test, the flame height was less than 150 mm within 60s. No flaming debris and glow were observed. Only whitish area was observed onto the surface at the end of the fire exposure. When the pilot flame was applied on the sample to know its surface spread flame behavior (BS 476 part-7), there was no charring on its surface even at the contact point of igniting flame. The spread of flame onto the surface of samples was not noticed even after 10 min exposure to radiant panel. Based on the observations, the sample classified as Class 1: surface of the very low spread of flame. Assessing the contribution towards fire growth, fire propagation index of the samples was calculated from the time-temperature data (BS: 476 Part-6). It was found that fire propagation index of the sample was <3 exhibiting negligible support to the fire growth.

Cone calorimetry results indicated that the samples exhibited negligible heat release (contribution in terms of heat released in the case of fire) and heat of combustion. The $CO_2$ yield (Kg/Kg) and CO yield (Kg/Kg) during exposure test were 0.43 and 0.023 respectively which were insignificant. The average mass loss rate (0.01 g/s) was also insignificant. It was concluded that foamed geopolymers exhibited satisfactory fire performance as observed from the flammability and reaction to fire characteristics test results.

Table 3 — Fire characteristics of the foamed geo polymers.

| Test | Value |
|---|---|
| • Reaction to fire characteristics | |
| - Ignitibility test (ISO 11925-2) | Class D (non-ignitable from edge as well as surface) |
| - Surface spread of flame (BS 476 part 5) | Class 1 |
| - Fire propagation index (BS 476 part 6) | < 3 |
| • Cone calorimetry (ISO 5660-2002) | |
| - Heat release rate (kW/m$^2$) | 2.1 |
| - Average mass loss rate (g/s) | 0.01 |
| - CO yield (Kg/Kg) | 0.023 |
| - $CO_2$ yield (Kg/Kg) | 0.43 |
| - Heat of combustion (mJ/Kg) | Negligible |

### 3.4 Leaching Behavior

One aspect of durability of geopolymer is its long term stability against the aqueous leaching of constituents when subjected to wet environment. Doubts are often raised on the leaching of salts precipitated during geopolymerization process giving rise to an efflorescence issue[40]. When the samples were immersed in water, the pH of water suddenly increased at 10.5 after 15 min as expected followed by its leveling off with further increasing time (Fig. 12). The maximum pH of the leached water was 12.2. As dissolution proceeds, the reaction slows down because of a back reaction which tends to precipitate some of the dissolved species giving rise to slightly decline in pH. It was also noted that the foamed geopolymers displayed higher alkaline character of leachates (pH 11-12.2) than those of corresponding un-foamed and raw fly ash (pH ~8.2). During TCLP test (pH 5), the concentrations of Na-ions in the leached water were ~22 ppm

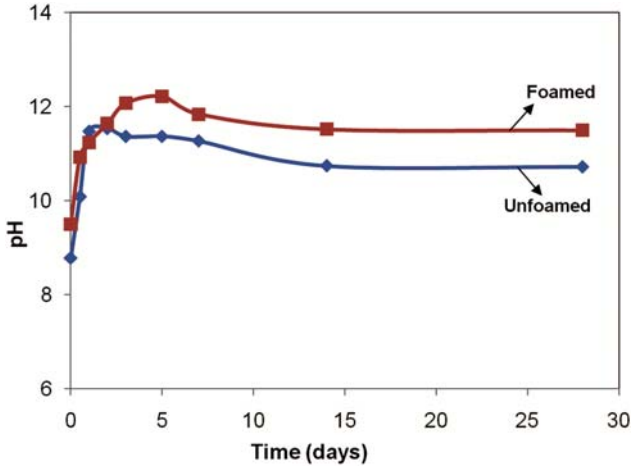


Fig. 12 — pH of leached water from the foamed/un-foamed geopolymers as a function of immersion time.

attributable to the diffusion of pore water from the geopolymers into the solution and its framework dissolution by $Na/H_3O^+$ ion exchange[41]. Si releases were ~18 ppm probably due to the un-polymerized silica as well as solubility of some silicon from the geopolymer framework[42]. The Al releases were very low (0.18 ppm) as compared to Na and Si probably due to the solubility constraints of amorphous[43] $Al(OH)_4$. The leachable levels of Fe remained very low (0.053 mg/l). It is reported[44] that Fe in the fly ash is mainly present as magnetite mixed with hematite. Their spinel structures are highly stable and therefore Fe and any isomorphously substituted elements were not easily released to the environment.The fly ash has also slow dissolution rate of its crystalline aluminosilicate constituent[45]. The estimated concentrations of Al and Fe were in compliance with the limit value of TCLP (Al: 0.05-0.2 and Fe: 0.3 mg/l). The release of sodium and calcium into the leached water was also in the permissible limits mentioned for drinking water. Based on the pH value, it was observed that geopolymeric products are resistant to aqueous leaching satisfying their use in wet environment.

### 3.5 Production of Blocks/Bricks

The foamed geopolymer blocks of size 280 mm x 180 mm x 130 mm were produced by *in-situ* method using fly ash/slag blend, alkaline activator (45-48 wt%, sodium hydroxide and sodium silicate in a mass ratio of 1:2.5),$H_2O_2$ (1-2 wt%), sodium lauryl sulphate (0.15-0.3 wt%) and sodium silicofluoride (~3 wt%). The general properties of foamed geopolymer blocks are given in Table 4. It was observed that the surfaces of blocks were smooth and free from any ridges or depressions (Fig. 13). The oven dry densities of blocks were in the range of 800 to 1000 kg/m$^3$. These blocks had compressive strengths varied from 4.2 to 6.5 MPa. The drying shrinkage of blocks was ~0.04% only when compared with the specified value of 0.08% for cellular concreteblocks[26]. The foamed geopolymer blocks satisfied the requirements mentioned in the commercial specification of the cellular/aerated concrete blocks of the same density (IS: 2185, 2008[26]). It can be considered as roof deck blocks and non-load bearing walls in RCC/steel framed structures. In another attempts, the light-weight bricks of size 2300 mm x 1150 mm x 750 mm were also produced from the foamed geopolymers. The de-moulded bricks exhibited open coarse texture. The foamed bricks had a density of ~ 800 kg/m$^3$ with a compressive strength of 4-5 MPa. It can be used for insulation and non-load bearing purposes.

Table 4 — Comparative properties of foamed geo polymer blocks and cellular concrete blocks.

| Property | Foamed geo polymer blocks | Cellular concrete blocks (IS 2185 part 4, performed) | Autoclave aerated concrete blocks (IS 2185 part 3) |
|---|---|---|---|
| Density (kg/m$^3$) | 800-1000 | 800-1000 | 800-1000 |
| Water absorption (%, 24h) | 6.1-11 | 12.5 | - |
| Compressive strength (MPa) | 4.2-6.5 | 2.5-3.5 | 6-7 |
| Thermal conductivity (W/m.K) | 0.19-0.23 | 0.32-0.30 | 0.37-0.42 |
| Drying shrinkage (%) | 0.04 | 0.08 | .05-0.1 |

Fig. 13 — Production of the foamed geopolymer concrete blocks.

## 4 Conclusions

Results indicate that foamed geopolymers produced by *in-situ* method have considerable potential in building industry for making building blocks for non-load bearing applications. The foam was in a pourable state at the time of placement. The superior calorimetric response of foamed geopolymer in comparison to its un-foamed counterparts is attributed to the exothermic reaction occurred between the sodium hydroxide of the activating

solution and hydrogen peroxide giving rise to more reaction product formation. The thermal conductivity of foamed geopolymers was superior to cellular concrete by differing in cellular morphology. From the fire point of view, the foamed geopolymer did not support any fire growth/flame spread because of its aluminosilicate character. Leachability studies indicated that the alkali-rich leachates for foamed geopolymers were higher than the un-foamed specimens because of their higher porosity and salt deposition into the pores. The release of Na and Si ions was predominant into leached water due to the dissolution of Na ion from the deposits existed in the pores, soluble silica from un-utilized sodium silicate and also from the framework dissolution. The developed foamed geopolymer blocks exhibited comparable properties as specified in the commercial specification for preformed foam/autoclaved cellular concrete blocks. Understanding on the control of cellular structures in the foamed geopolymers is necessary through the use of surfactant and setting hardener during the foaming process to obtain acceptable physico-mechanical properties of the products without any efflorescence.

## Acknowledgements

This paper forms part of a supra institutional project of the CSIR R&D program (Govt. of India) and is published with permission of the Director, CSIR-Central Building Research Institute, Roorkee, (India). One of the authors is thankful to Uttarakhand Technical University, Dehradun for registering as a PhD candidate.

## References

1 Zhang Z, Provis J L, Reid A & Wang H, *Constr Build Mater,* 56 (2014) 113.
2 American Concrete Institute (ACI-523), *Guide for cast-in-place low density cellular concrete, ACI 523-1R*, USA (2006).
3 Neville A M, *Properties of Concrete,* 5th ed (Pearson Education Ltd. India), (1995) 688, ISBN No.: 978-0-273-75580-7.
4 Kearsley E P & Wainwright P J, *Cem & Concr Res,* 32 (2002) 233.
5 Feng J, Zhang R, Gong L, Li Y, Cao W & Cheng X, *Mater Des,* 65 (2015) 529.
6 Davidovits J, *J Therm Anal,* 37 (1991) 1633.
7 Singh B, Ishwarya G, Gupta M & Bhattacharyya S K, *Constr Build Mater,* 85 (2015) 78.
8 Zhang Z, Wang H, Reid A & Aravinthan T, *In: incorporating Sustainable Practice in Mechanics of Structures and Materials*, ACMSM21, CRC press, Taylor Francis Group, Melbourne, (2010) , ISBN No.: 9780203829868.
9 Al Bakri Abdullah M M, Hussain K, Binhussain M, Ismail K N, Yahya Z & Razak A R, *Intl J Mol Sci,* 13 (2012) 7186.
10 Abdollahnejad Z, Pacheco-Torgal F, Felix T, Tahri W & Aguiar J B, *Constr Build Mater,* 80 (2015) 18.
11 Boke N, Brich D G, Nyale M S & Petrik F, *Constr Build Mater,* 75 (2015) 189.
12 Papa E, Medi V, Kpogbemabou D, Moriniere V, Laumonier J, Vaccari A & Rossignol S, *Energy Build,* 131 (2016) 223.
13 Bai C & Colombo P, *Ceram Intl,* 43 (2017) 2267.
14 Hajimohammadi A, Ngo T, Mendis P, Nguyen T, Kashani A & Van Deventure J S J, *Mater Des,* 130 (2017) 381.
15 Kovalchuk G & Krivenko P V, Producing Fire and Heat Resistance Geopolymers. In: Povis J L & van Deventure J S J, *Geopolymers : Structure, Properties and Industrial Applications*, Woodhead, Cambridge, (2009) 227, ISBN No.: 978-1-84569-449-4.
16 Nair B G, Zhao Q & Cooper R F, *J Mater Sci*, 42 (2007) 3083.
17 Richard W A, Williams R, Temuujin J & Van Riessen A, *Mater Sci Eng,* 528 (2011) 3390.
18 Papakonstantinou C G, Giancaspro L W & Balaguru P N, *Compos Part A,* 39 (2008) 75.
19 Lyon R E, Balaguru P N, Foden A J & Davidovits J, *Fire Mater,* 21 (1997) 61.
20 Musci G, Szenzi A, Mohnar Z & Lakatos J, *J Environ Eng Landscape Manag*, 24 (2016) 48.
21 Temuujin J, Minjigmaa A, Lee M, Chen-Tan N & Van Riessen A, *Cem Concr Compos,* 33 (2011) 1086.
22 Izquierdo M, Querol X, Davidovits J, Antenucci D, Nugterend H & Fernandez Pareira C, *J Hazard Mater,* 166 (2009) 561.
23 Van Jaarsveld J G S, Van Deventur J S J & Lorenzen, *Miner Eng,* 12 (1999) 75.
24 *Indian Standards for Pulverized Fuel Ash Specification, Part 1: For Use As Pozzolana in Cement, Cement Mortar and Concrete,* Bureau of Indian Standards *(IS: 3812-1) (2003), New Delhi.*
25 Singh B, Rahman M R, Paswan R & Bhattacharyya S K, *Constr Build Mater,* 118 (2016) 171.
26 *Indian Standards for Concrete Masonry Units, Part 4: Preformed Foam Cellular Concrete Blocks,* Bureau of Indian Standards (*IS: 2185-4) (2008)*, New Delhi.
27 Bai C, Franchin G, Elsayed H, Conte A & Colomo P, *J Eur Ceram Soc*, 36 (2016) 4243.
28 Novais R M, Buruberri L, Ascensco G & Seabra M, *J Clean Prod,* 119 (2016) 99.
29 Toxicity Characteristic Leaching Procedure (TCLP), *US Environmental Protection Agency,* EPA 1311, (1992).
30 *Indian standard Method for the Determination of Thermal Conductivity of Thermal Insulation Materials (two slab, guarded hot-plate method),* Bureau of Indian Standards, (*IS 3346) (1990),* New Delhi.
31 *Indian Standards, Methods of Test For Pozzolanic Materials*, Bureau of Indian Standards, (*IS 1727) (1999),* New Delhi.
32 Vol'nov I I & Shatunina A N, *Acad Sci,* 12 (1963) 185.
33 Hao L, Wang R & Zhang L, *Cellulose,* 21 (2014) 777.
34 Vaou V & Panias D, *Miner Eng,* 23 (2010) 1146.
35 Rice R, *J Mater Sci,* 31 (1996) 1509.

36 Garcia-Lodeiro I, Fernandez-Jimenez A & Palomo A, *J Am Ceram Soc,* 93 (2010) 1934.
37 Prud'homme E, Michaud P, Joussein E, Clacens J & Rossignol S, *J Non Crys Solids,* 357 (2011)1270.
38 Macphee D E, Luke K, Glasser F P & Lachowski E E, *J Am Ceram Soc,* 72 (1989) 646.
39 Demirboga R, *Build Environ,* 42 (2007) 2467.
40 Zhang Z & Provis J L, *Cem Concr Res,* 64 (2014) 30.
41 Aly Z, Vance ER, Perera D S, Hanna JV, Griffith CS, Davis J & Durce D, *J Nucl Mater,* 378 (2008) 172.
42 Fruchter J S, Rai D & Zachara J M, *Environ Sci Tech,* 24 (1990) 1173.
43 Warren C J & Dudas M J, *Total Environ,* 83 (1989) 99.
44 Izquierdo M & Querol X, *Intl J Coal Geo,* 94 (2012) 54.
45 Kulier U, Ishak C F, Sumner M E & Miller W P, *Environ Pollut,* 123 (2003) 255.